Design, Trajectory Generation and Control of Quadrotor Research Platform

Durgesh Haribhau Salunkhe , Siddhant Sharma , Sujal Amrit Topno , Chandana Darapaneni
Amol Kankane and Suril V Shah

***Abstract*— We describe the modeling, estimation and control of a quadrotor in 3D environment using the 3DR Pixhawk PX4 as controller through Robot Operating System(ROS). The paper discusses a method to measure moment of inertia of quadrotor about its principal axes to achieve better results in an inexpensive way. We also present the trajectory generation and segment optimization of the trajectory commanded to the quadrotor. We describe a method of controlling the quadrotor through ROS by providing necessary inputs to the flight controller using the built-in firmware.**

I. INTRODUCTION

In the recent decade there has been a rise of interest in quadrotors and its control. Quadrotors consist of four propellers having fixed-pitch blades, attached to motors mounted on a rigid cross frame configuration. Vertical Take-Off and Landing (VTOL) and hovering like a conventional helicopter is one of the major benefits of such multirotor platforms [1]. Few applications of quadrotors include search and rescue [2], surveillance [3], reconnaissance and data acquisition. Various peripheral devices can be mounted on the quadrotor as per the required application. Quadrotors are simple to model as no swash-plate mechanism is required. Being under-actuated, the dynamic model of a quadrotor consists of non-linear and multivariate equations. To have a better control over quadrotors, it is very important to have accurate values of physical parameters. The inertia along principal axes is either calculated theoretically [4] or by modeling in CAD softwares. The inertia values calculated by this method may deviate from the actual performance due to assumptions and mistakes in CAD modeling.

Trajectory generation of the quadrotor is based on optimizing the input parameters. [5] and [6] have proposed a cubic polynomial trajectory or a minimum acceleration trajectory. [7] discusses about minimum jerk trajectory and its performance with quadrotors. Though these trajectories create a smooth path, the optimizing parameter of the quadrotor is snap, the fourth derivative of position. The minimum snap trajectory generates smooth transition through given set of waypoints [8]. Trajectory is controlled by feeding necessary inputs which are a function of time. Robust flight controllers are available which allow us to follow the generated trajectories with accuracy.

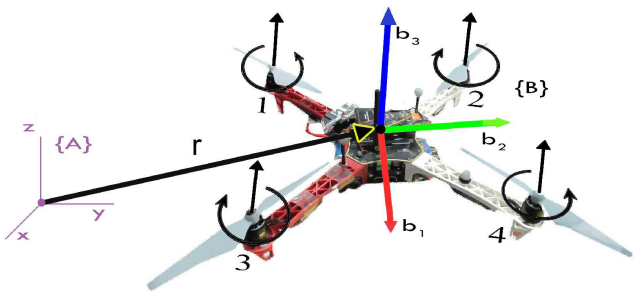

Fig. 1: Quadrotor build and frames in 'X'-configuration

3DR Pixhawk v2 PX4 is one of such flight controllers. Pixhawk provides real time flight data transmission, suitable for both research as well as on-field applications. The open source firmware provided by Pixhawk is continuously upgraded by a large community of developers. Research based on open source platforms prevents one from wasting effort on work already achieved. Control of an open source platform, Mikrokopter, has been reported earlier [1]. Implementation of common robotic algorithms is simplified using ROS. The data streaming and communication with Flight Control Unit (FCU) is done using the MAVLink protocol.

Various methods for outdoor as well as indoor state estimation have been explored so far. The work reported was performed in a laboratory setup and so the quadrotor was maneuvered in a constrained and well defined space. We use VICON motion capture system to estimate the state of the quadrotor. VICON is a vision-based global localization system. It serves the purpose of estimating all states required to control a quadrotor. This system is reliable and provides an accurate estimation of the quadrotor.

We propose a method that enables us to get accurate values of moment of inertia in a safe and inexpensive

This work was supported by Suril Shah, Asst. Prof, IIT Jodhpur, Rajasthan.

Durgesh Haribhau Salunkhe, Siddhant Sharma and Sujal Amrit Topno are Undergraduate Students at Birla Institute of Technology, Mesra, Ranchi salunkhedurgesh@gmail.com

Chandana Darapaneni is an Undergraduate Student at Indian Institute of Technology, Jodhpur, Rajasthan

Amol Kankane is an Undergraduate Student at Indian Institute of Technology(BHU) Varanasi

Suril V Shah is a Faculty member, Mechanical engineering, Indian Institute of Technology,Jodhpur.

manner. A method of tuning gain values for roll and pitch of the quadrotor is also mentioned. The relation of thrust and reaction moment with the rpm of motors is calculated by using momentum theory [9]. An experimental setup is proposed to measure the proportionality constants. We generate minimum snap trajectory and also propose a method to optimize segment time allocation for the trajectory. Control of the quadrotor from Robot Operating System (ROS) using the MAVROS package on an off board computer is also discussed in the paper.

Section II discusses the design considerations of the quadrotor. The measurement of the parameters related to dynamic modeling of the quadrotor are also detailed in this section. In Section III the dynamic modeling and linear control of the quadrotor has been described along with trajectory generation and segment optimization. In Section IV, the paper details the flight controller used and the state estimation of a quadrotor using VICON, it also explains the communication by use of ROS. We present our results in Section V and put forward future work in Section VI.

II. DESIGN CONSIDERATIONS

A quadrotor has to be chosen with all considerations related to the application for which it is used. We explain the design process of selecting components and contribution of each component in the performance of the quadrotor.

A. Design of the Quadrotor

We built a quadrotor which followed a particular given trajectory while carrying a considerable payload such as a manipulator [13] or any other sensor like laser scanner [14] which are extensively used in research on quadrotor. The process of selecting the components is described in Fig. 2. The deciding parameters were payload and the endurance of the quadrotor. The weight of the quadrotor built is 1.12 kg and has flight time of 7 minutes with a 3S 4000 mAh Lithium Polymer (LiPo) battery. The quadrotor can carry a payload of maximum 900 grams. The size of the frame is 450mm measured diagonally. Z-blade propellers of 9.4 inch diameter with a pitch of 5 inch are used to achieve a thrust to weight ratio of 2.1. The quadrotor was optimized in terms of its maneuvering capabilities and payload capacity. We chose Pixhawk V2 PX4 as our flight controller due to its advantages discussed in Section IV. Preliminary calculations were done to calculate thrust to weight ratio, flight time and angular acceleration of the quadrotor.

B. Measurement of Thrust and Reaction Moment

We calculated the maximum thrust and reaction moment provided by the motors. The thrust was estimated theoretically, using momentum theory. The relation of thrust and the reaction moment is proportional to ω^2. We estimated the coefficients that related thrust and reaction moment with the square of the angular velocity of the motors. These experiments were performed in order to have a better control over the dynamics of the quadrotor.

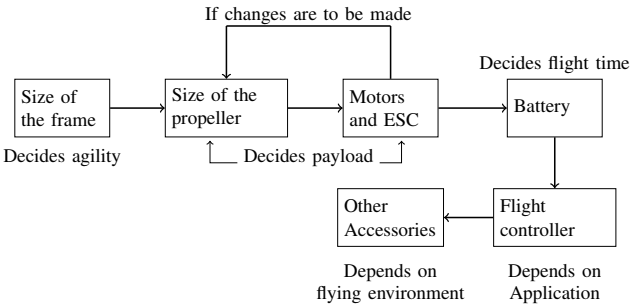

Fig. 2: Design process for component selection

The proportionality constants K_t and K_m are the prime parameters to be measured. The actual net thrust and moments provided by the rotors were calculated by the experimental setup in Fig. 3 and 4. For the experiment, an L-shaped rigid structure made of wood was pivoted at the intersection of the arms. A weighing pan was placed under one arm to measure the thrust. The motor was mounted in such a manner that the thrust generated reflected as weight on the weighing pan as shown in Fig. 3. A laser tachometer was used to estimate the rpm of the motor. The thrust measured was tabulated against ω^2.The formula used :

$$K_t = \frac{W l_1}{l_2\ \omega^2} + c_1 \tag{1}$$

Where W is the force exerted on the weighing scale measured in Newtons. c_1 is the constant that showed the offset of the actual result from the one expected. The average was taken and value of K_t was calculated as 1.10×10^{-7} and c_1 was approximately 1.10×10^{-3}

For the computation of K_m, the motor was mounted on the adjacent face of the wooden block as shown in Fig. 4. The moment was calculated by measuring the force on the weighing pan. The reaction moment was plotted against the square of angular velocity. K_m was calculated using the following relation:

$$K_m = \frac{W l_1}{\omega^2} + c_2 \tag{2}$$

Where $l_1 = l_2 = 18cm$, is length of the arms of the structure used. The average K_m came out to be = 2.94×10^{-9} without any offset (c_2 = 0).

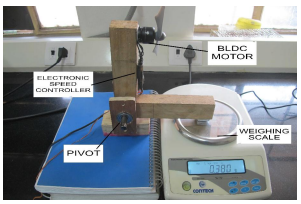

Fig. 3: Setup for measuring thrust

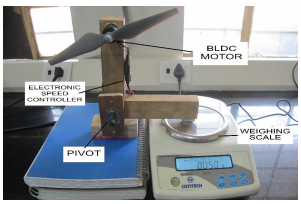

Fig. 4: Setup for measuring reaction moment

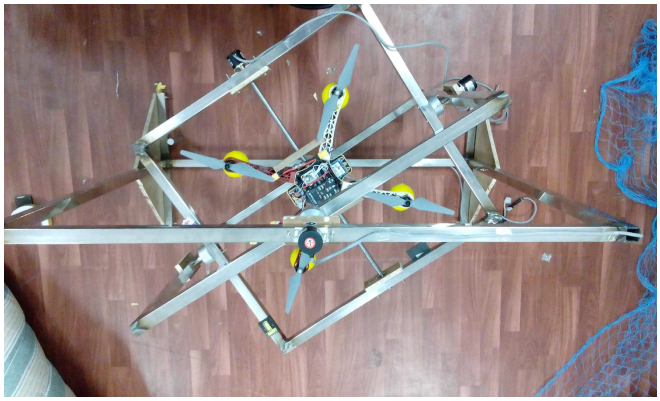

Fig. 5: Top view of test rig showing 3 DOFs

C. Measurement of Inertia Tensor

In order to measure the next set of parameters as per required applications, a test rig was designed, shown in Fig. 5. We measured the moment of inertia along the principal axes and tuned the gain values for roll and pitch angles using the mentioned test rig. A test bench that measures all 6 DOFs of the quadrotor has been built by [15]. Though the test bench is capable of measuring all DOFs, the cost of such test benches is high. While using a ball joint mechanism, the roll and pitch axes don't necessarily pass through the center of gravity of the quadrotor which may create an error in the result. The proposed test rig is capable of measuring all the rotational DOFs in an inexpensive manner. It consists of three frames forming a gimbal, a mechanism that has three rotational degrees of freedom. The experiments were performed with the quadrotor mounted on the test rig about the pitch axis. The shaft that extended from quadrotor passed through the center of gravity of the quadrotor which helped in reducing the errors in tuning of the quadrotor. Optical shaft encoders with a resolution of 0.02 degrees were used to measure the rotations about the 3 axes.

Moment of inertia of the quadrotor is an important parameter that directly governs the control of quadrotor. Most of the literature currently available focuses on measuring I_{xx}, I_{yy} and I_{zz} theoretically [4] or by the use of CAD softwares. Use of CAD requires a detailed design of the Quadrotor in the software for accurate figures to be achieved. In our approach we used the test rig to measure the values of I_{xx} and I_{yy} experimentally. We mounted the quadrotor in the test rig as described and rotated motor 1 and 3 shown in Fig. 1 which would provide pitching of the quadrotor. The quadrotor was held stationary with the motors 1 and 3 (Fig.1) rotating till a constant rpm of motors was measured and then the quadrotor was set free to rotate. We obtained the plot of angular velocity of the rotating quadrotor against time. The quadrotor accelerated initially to attain a constant angular velocity as shown in Fig. 6. This accounts to the drag forces acting on the quadrotor. These forces also contribute in the angular acceleration for pitching. As these forces are not calculated, the theoretical relation of Moment and the angular acceleration do not hold true. In the experiment performed, we estimated near to actual relation of moment and angular acceleration of the quadrotor. The moment was calculated from the thrust corresponding to the rpm of the motors from previous experiment. Angular acceleration (α) was obtained as the slope of ω v/s time graph till the red line shown in Fig. 6. The inertias were then calculated by using the relation between the moments and angular acceleration achieved.

$$M = K_t \omega^2 \times \frac{L}{\sqrt{2}} \times 2 \tag{3}$$

$$\alpha = \frac{\omega}{t} \tag{4}$$

$$I_{xx,yy} = \frac{M_{x,y}}{\alpha_{x,y}} \tag{5}$$

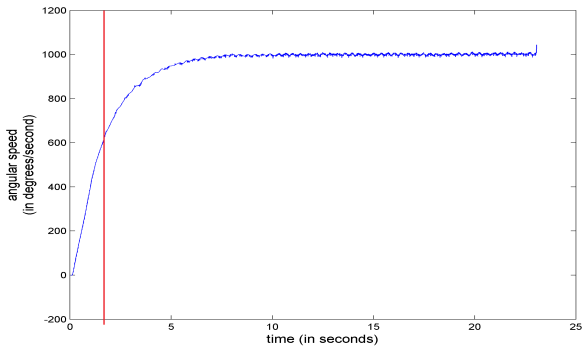

Fig. 6: Plot of angular speed vs time for measuring I_{xx}

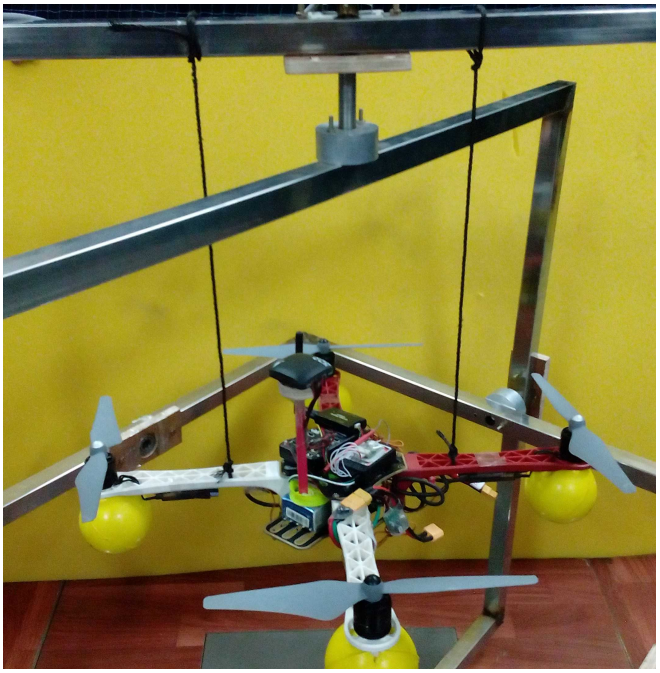

Fig. 7: Quadrotor suspended for measuring I_{zz}

In general I_{zz} is approximated to be the sum of I_{xx} and I_{yy}. We used the concept of bifilar pendulum to measure Izz. Two vertical strings were used to suspend the quadrotor in horizontal position as shown in Fig. 7. On giving a small angular displacement about the yaw axis. The quadrotor exhibits oscillations. The moment of inertia can be measured using the equation:

$$I_{zz} = \frac{mg\ T^2 d^2}{4\pi^2 l} \tag{6}$$

Where, T is the time period oscillations, $2d$ is the distance between two string, and l is the length of the strings. Here, we measured $T = 1.65sec$, $l = 0.38m$ and $d = 0.105m$.

$$I_{zz} = 0.022kgm^2$$

The test rig was also used to tune gain values for the pitch and roll control. Pixhawk Ground Control Station(GCS) provided the flexibility of tuning the K_p, K_d and K_i values of roll, pitch and yaw movements. Pitch angle was given to the quadrotor mounted on the test rig using the transmitter radio and data from the encoders was used to decide over the gain values. We adopted Ziegler - Nichols rule for tuning the gain values. K_d and K_i were reduced to zero. The K_p was increased from zero, until a point where stable oscillations were observed. K_i was decided according to the heuristic method till the maximum value of K_p to avoid the steady state error in the quadrotor. K_d, which governs the damping in error correction was tuned by the same method till an optimum value was achieved. Same process was adopted for tuning the gains for roll. The quadrotor was mounted in such a manner that the roll axis coincided with the previous pitch axis. This was done in order to avoid the effect of the inertia of the frame of the test rig.

III. MODELLING AND CONTROL

There were two possible configurations of the quadrotor to be chosen from viz. '+' configuration and 'X' configuration. In a '+' configuration, the roll and pitch axes are along the arms of the quadrotor whereas in an 'X' - configuration the roll and pitch axes are shifted 45 degrees from the arms of the quadrotor. We preferred 'X' configuration over '+' configuration as the 'X' configuration had advantages in dynamics over the other configuration. In 'X' configuration all the 4 motors are responsible for roll and pitch control. This gives a thrust advantage over the other configuration by a factor of $\sqrt{2}$. Also, the configuration allows better use of sensors or cameras as the propellers don't interfere in the line of sight. As the quadrotor is expected to carry a payload, it is always an advantage to have extra thrust in control.

The coordinate systems including the world frame A and the body fixed frame B are shown in Fig. 1. We use $Z-X-Y$ Euler angles to define the $Roll(\phi)$, $Pitch(\theta)$ and $Yaw(\psi)$ in the local coordinate system. The rotation matrix for the transformation from body fixed frame to the world frame is given by:

$${}^{A}R_{B} = \begin{bmatrix} c\psi c\theta - s\phi s\psi s\theta & -c\phi s\psi & c\psi s\theta + c\theta s\phi s\psi \\ c\theta s\psi + c\psi s\phi s\theta & c\phi c\psi & s\psi s\theta - c\psi c\theta s\phi \\ -c\phi s\theta & s\phi & c\phi c\theta \end{bmatrix}$$

The linear accelerations in x, y and z directions can be written as:

$$\ddot{x_{des}} = g(\theta_{des}\cos\psi_T + \phi_{des}\sin\psi_T) \tag{7}$$

$$\ddot{y_{des}} = g(\theta_{des}\sin\psi_T - \phi_{des}\cos\psi_T) \tag{8}$$

$$\ddot{z_{des}} = \frac{1}{m}u_1 - g \tag{9}$$

By applying PD controller to 7, 8 and 9 , we get,

$$\ddot{x_{des}} = \ddot{x}_T + k_{d,x}(\dot{x}_T - \dot{x}_{current}) + k_{p,x}(x_T - x_{current}) \tag{10}$$

$$\ddot{y_{des}} = \ddot{y}_T + k_{d,y}(\dot{y}_T - \dot{y}_{current}) + k_{p,y}(y_T - y_{current}) \tag{11}$$

$$\ddot{z_{des}} = \ddot{z}_T + k_{d,z}(\dot{z}_T - \dot{z}_{current}) + k_{p,z}(z_T - z_{current}) \tag{12}$$

$$\begin{aligned} u &= mg + m\ddot{z}_{des} \\ &= mg + m(\ddot{z}_T + k_{d,z}(\dot{z}_T - \dot{z}_{current}) + k_{p,z}(z_T - z_{current})) \end{aligned} \tag{13}$$

u represents the thrust applied by all the four motors of the quadrotor. The roll(θ), pitch(ϕ) and yaw(ψ) angles are calculated as following:

$$\phi_{des} = \frac{1}{g}(\ddot{x}_{des}\sin\psi_T - \ddot{y}_{des}\cos\psi_T) \tag{14}$$

$$\theta_{des} = \frac{1}{g}(\ddot{x}_{des}\cos\psi_T - \ddot{y}_{des}\sin\psi_T) \tag{15}$$

$$\psi_{des} = \psi_T(t) \tag{16}$$

The subscripts T, des and current denote given trajectory, desired and current states respectively.
The values of roll(θ), pitch(ϕ), yaw(ψ) angles and the thrust was calculated from the control equations. Pixhawk takes θ, ϕ, ψ and thrust as inputs and achieves the desired control.

A. Trajectory generation

A 3 waypoints trajectory was given to the quadrotor. The time alloted to the trajectory was sufficient so that the quadrotor could follow it by implementing linear control.Maneuvering of the quadrotor is achieved by changing the angular velocities of the motors which result in the angular acceleration of the quadrotor about its principal axes. In Section III it was shown that $\phi \propto \ddot{y}$ As the change in angular velocity of motors results in $\ddot{\phi}$, the natural choice of optimal function is the fourth derivative of position(y^{iv}) also called as jounce or snap. Minimum jerk trajectories have been tried for quadrotor [7] but the optimization of input parameters can be justified with a minimum snap trajectory only [8].
The trajectory was written in piecewise polynomial, by ensuring that the trajectory between two consecutive waypoints is a minimum snap trajectory.

$$f(t) = min \int_0^t |x^{(iv)}|^2, |y^{(iv)}|^2, |z^{(iv)}|^2, |\ddot{\psi}|^2.dt \tag{17}$$

by Euler Lagrange method, the optimal function has to satisfy the following condition:

$$\frac{\partial L}{\partial m}-\frac{d}{dt}\left(\frac{\partial L}{\partial \dot{m}}\right)+\frac{d^2}{d^2t}\left(\frac{\partial L}{\partial \ddot{m}}\right)-\frac{d^3}{d^3t}\left(\frac{\partial L}{\partial \dddot{m}}\right)+\frac{d^4}{d^4t}\left(\frac{\partial L}{\partial m^{iv}}\right)=0 \tag{18}$$

The optimal function, $L=f(m,\dot{m},\ddot{m},\dddot{m},m^{(iv)},t)$. $f(t)$ is a seven degree polynomial. There are 8 unknown co-efficients for each segment, these co-efficients were solved by initial and final boundary conditions and equating the values till 6^{th} derivative of $f(t)$ at the intersection of two segments.

B. Segment time optimization

As the quadrotor started, passed through a ring and then stopped, our trajectory had 3 waypoints and 2 segmented trajectories. The time was initially alloted proportional to the distance between waypoints.

$$T_i=\frac{w_{i+1}-w_i}{k} \tag{19}$$

In the above equation, the value of k decided the speed of the trajectory. The given trajectory can be followed The waypoints were defined and the trajectory time was specified. This case allowed us to optimize the segment time allocation. The segment time(T_1 and T_2) were re-allocated by giving T_1 an additional time and subtracting same amount of time from the next segment.

$$T_{1new}=T_1+t'$$

$$T_{2new}=T_2-t'$$

t' was iterated within a range of value which kept the speed of trajectory under 1m/s and the optimization parameter was the total distance traveled by quadrotor.

$$f(T_{1new},T_{2new})=min\sum_0^t(|x|+|y|+|z|) \tag{20}$$

subject to conditions:

$$t'<T_1$$

$$\frac{w_2-w_1}{T_{1new}},\frac{w_3-w_2}{T_{2new}}<=1$$

The time was optimized only for trajectories with 2 segments but trajectories with more segments can be optimized if the segments are seperated in pairs.

IV. Implementation through ROS

The section describes the flight controller used in details. Communication by using ROS and implementation of the same to follow a given trajectory is also mentioned.

A. Flight Controller- Pixhawk

Pixhawk is a powerful 32-bit ARM architecture based micro-controller having failsafe backup controller and extensive memory. No special controller designing is required for researchers concentrating on navigation control and path planning applications [16]. It is easy to stream data, to and from Pixhawk through MAVLink protocol using Robot Operating System (ROS), [17], due to availability of the precompiled packages such as MAVROS.

The MAVLink protocol is also supported in the form of MATLAB packages enabling a direct control of the quadrotor, Fig. 8 shows the proposed forms of data flow for *Pixhawk*.

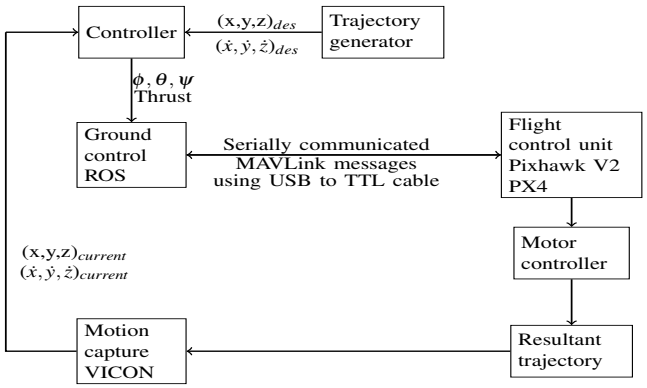

Fig. 8: Proposed Experimental Setup

B. Sensors and Feedback

The pixhawk flight controller is equipped with advanced multiple sensors to enable accurate pose estimation of the quadrotor. It employs homogeneous as well as heterogeneous fusion of sensors to make the resultant data more dependable and accurate. There is homogeneous fusion amongst the two gyroscopes and two accelerometers provided and a heterogeneous fusion amongst all 3-axis gyroscopes, accelerometers, magnetometer and with single axis barometer to yield a *10 DOFs* Inertial Measurement Unit (IMU). The two accelerometers and gyroscopes also provide Pixhawk with failsafe capabilities.

C. Offboard control using ROS

A ROS network consisting of the following systems was setup using 'MAVROS' & 'vicon_bridge' packages of ROS as shown in Fig. 10.

1) Sensor Data (from mavros package)
2) Controller (Roll-Pitch-Yaw-Thrust control)

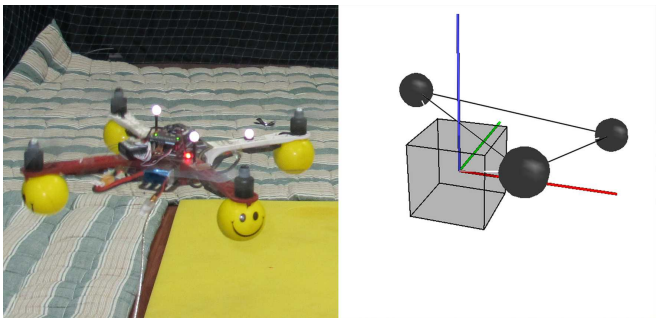

Fig. 9: Quadrotor with reflective IR markers(left) and object created in VICON environment(right)

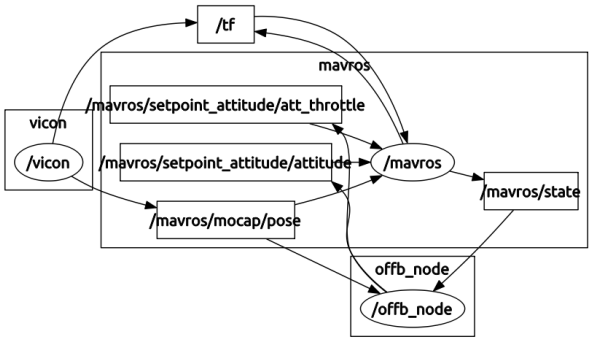

Fig. 10: Graph showing communication between the ROS nodes

3) Motion Capture feedback (vicon_bridge)

The VICON motion capture system (MOCAP) uses reflective markers to capture the locations. The Tracker 2.2 software used allowed us to use multiple markers collectively to make-up object(s) in order to track the pose of desired body accurately. The pose estimate was calculated as a weighted mean of the MOCAP and the internal IMU data. RPYT control was adopted to achieve a desired pose. The present and desired pose was known, thus establishing a closed loop PID control over its pose. The communication between the ROS computer and Pixhawk was first attempted using 433 MHz serial radio which showed latency in data transfer. Hence, a wired mode of communication using USB to TTL cable was implemented. The Fig. 10 shows that vicon MOCAP data was subscribed (received) by MAVROS using the /mocap/pose topic that enabled the fusion of the internal IMU and external MOCAP feedback. The offboard controller node (C++ code run in ROS) published (sent) attitude and throttle control over the setpoint_attitude topic. Fig. 9 shows the markers mounted on quadrotor and the markers detected in Tracker 2.2 using VICON motion capture system.

V. RESULTS AND DISCUSSIONS

The results obtained by the experimental setup are discussed in the following section. The plots of expected trajectory and the actual trajectory are also shown in the section.

A. Values of K_t and K_m

The plots of K_t and K_m against the square of the rpm of the motor is shown in Fig. 11 and Fig. 12. The plots clearly show that the thrust and the reaction moment are proportional to the square of angular velocity. This plot helps in directly calculating thrust or moment if the rpm of the motors is known.

B. Values of I_{xx}, I_{yy} and I_{zz}

The values of the moment of inertia about x-axis, y-axis and z-axis calculated with the test rig and CAD model are compared below.

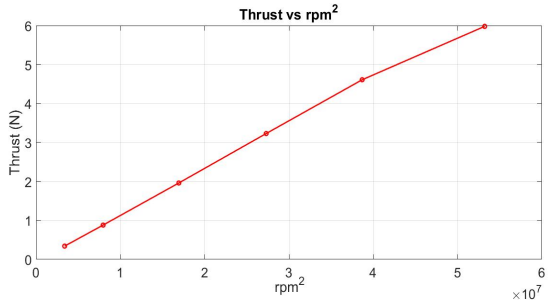

Fig. 11: Plot of Thrust vs square of Angular Velocity (ω^2)

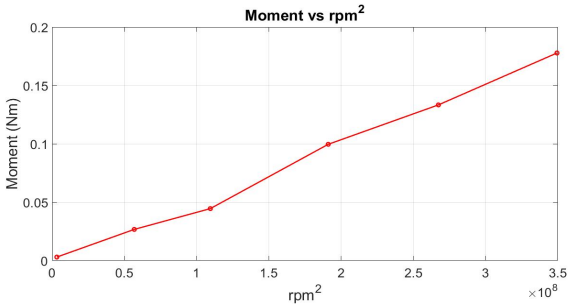

Fig. 12: Plot of reaction moment vs square of Angular Velocity (ω^2)

	Test rig, kg-m^2	CAD model, kg-m^2
I_{xx}	0.0157	0.01
I_{yy}	0.0134	0.011
I_{zz}	0.022	0.021

The values of I_{xx} and I_{yy} in CAD model are less than the test rig values and that can be expected due to the unaccounted drag forces acting on the quadrotor. The results show that the actual angular acceleration will be less than the calculated angular acceleration if the inertia is measured neglecting drag forces.The difference in value will increase as the size of quadrotor increases. I_{zz} on other side remains same in both methods. So, it can be concluded that the results obtained from the test rig are valid and using test rig is a better practice to measure inertia.

C. Trajectory segment time allocation

After the time alloted to each trajectory was optimised it was observed that the quadrotor traveled less distance than before. The paths are shown in fig. 14. The blue trajectory is a distance proportionate time alloted trajectory while the red plots are the trajectories with each iteration tried. The optimising parameter was the total distance traveled by the quadrotor. The plot in Fig. 14 shows the change in optimising function with iterations.

D. Trajectory traveled by the quadrotor

We were able to make the quadrotor follow a certain trajectory by giving RPYT as inputs to the flight controller. The desired path and the path traveled by the quadrotor is compared in Fig. 13. The Fig. 15 shows the composite image

of a quadrotor following the trajectory. The black cross marks are the waypoints in xy plane.

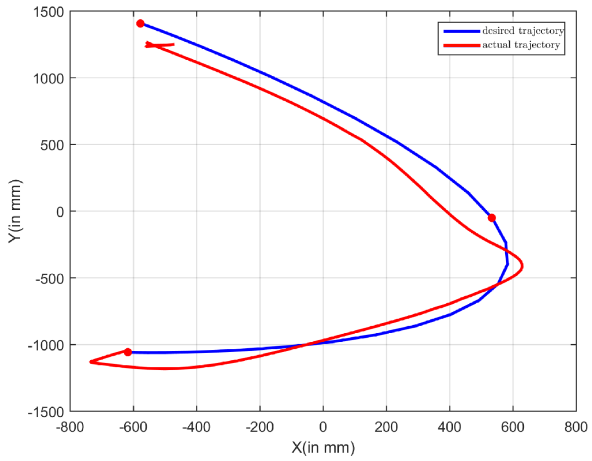

Fig. 13: Desired trajesctory and actual trajectory traveled by the quadrotor

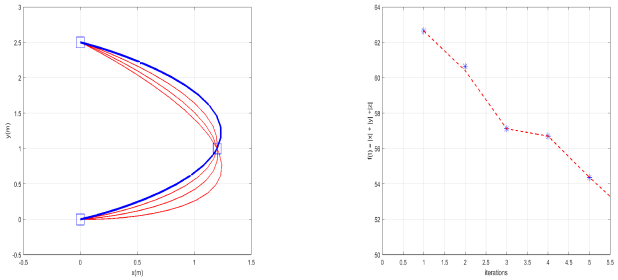

Fig. 14: The paths with iterations in t' and plot of optimised function vs iterations

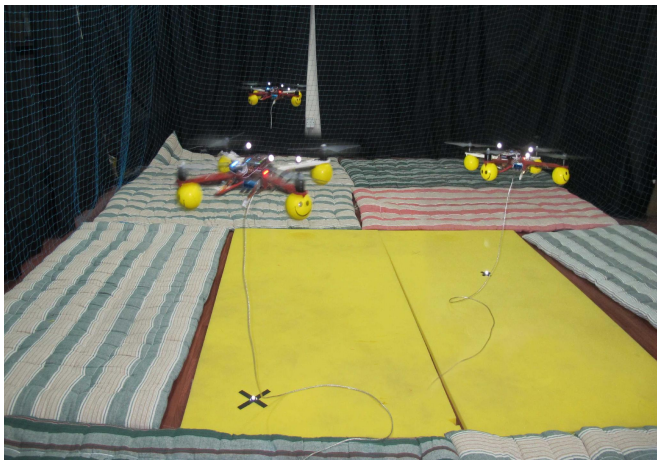

Fig. 15: Composite image of a single quadrotor traveling through given trajectory

VI. Conclusion and Future Work

In this paper we described methods to accurately measure the physical parameters that play an important role in dynamics. The methods mentioned are cost effective and ensure less errors. We also described trajectory generation & segment optimisation for a trajectory with 3 waypoints. We were successful in commanding a minimum snap trajectory through ROS by providing Roll, pitch and yaw angles and thrust value.

We are currently extending our methods of trajectory optimisation to trajectories with more segments. We are also exploring the firmware provided so that we can implement non linear control of the quadrotor in order to perform aggressive maneuvers.

References

[1] Inkyu Sa and Peter Corke, "Estimation and Control for an Open-Source Quadcopter" in *Proceedings of Australasian Conference on Robotics and Automation*, Dec, 2011

[2] Ryan, A., Hedrick, J. "A mode-switching path planner for UAVassisted search and rescue" in *44th IEEE Conf. Decision and Control, 2005 European Control Conference*, CDC-ECC 05, Seville, Spain, 2005.

[3] Alexis, K., Nikolakopoulos, G., Tzes, A., Dritsas, L. "Coordination of helicopter UAVs for aerial forest-re surveillance, in Applications of intelligent control to engineering systems", *Springer*, The Netherlands, 2009.

[4] Randal W.Beard, "Quadrotor Dynamics and Control.", February, 2008.

[5] Jong Tai Jang et.al "Trajectory Generation with Piecewise Constant Acceleration and Tracking Control of a Quadcopter", in *2015 IEEE*,

[6] "Trajectory generation and tracking using the AR.Drone 2.0 quadcopter UAV", in *12th Latin American Robotics Symposium and 2015 Third Brazilian Symposium on Robotics*, 2015

[7] Jing Yu, Zhihao Cai and Yingxum Wang ,"Minimum Jerk Trajectory Generation of a Quadrotor Based on the Differential Flatness", in *IEEE Chinese Guidance, Navigation and Control Conference*, 2014.

[8] Daniel Mellinger and Vijay Kumar, "Minimum Snap Trajectory Generation and Control for Quadrotors", in *IEEE International Conference on Robotics and Automation* 2011, Shanghai, China

[9] J. Leishman. "Principles of Helicopter Aerodynamics (Cambridge Aerospace Series)". *Cambridge, MA: Cambridge Univ. Press.* [Online]. Available: http://books.google.com.au/books?id=nMV-TkaX-9cC

[10] S. Shen, N. Michael, and V. Kumar. "Autonomous multi-oor indoor navigation with a computationally constrained MAV" in *Proc. of the IEEE International Conference on Robotics And Automation*, pages 2025, Shanghai, China, May 2011.

[11] S. Shen, Y. Mulgaonkar, N. Michael and V. Kumar. Vision-based state estimation and trajectory control towards high speed flight with a quadrotor.

[12] Ahmed Hussein, Abdulla Al-Kaff, Arturo de la Escalera and Jos Mara Armingol Intelligent Systems Lab (LSI) Research Group Universidad Carlos III de Madrid (UC3M), Leganes, Madrid, Spain. Autonomous Indoor Navigation of Low-Cost Quadcopters

[13] Hyunsoo Yang and Dongjun Lee, "Dynamics and Control of Quadrotor with Robotic Manipulator", in *IEEE International Conference on Robotics & Automation (ICRA)* ,Hong Kong, China, 2014.

[14] Xiang He, Zhihao Cai and Ruyi Yan, "A Quadrotor Helicopter Localization Method Using 2D Laser Scanner in Structured Environment", 2013

[15] Yushu Yu, Xilun Ding. "A Quadrotor Test Bench for Six Degree of Freedom Flight" in *Journal of Intelligent Robotic System*, 2012.

[16] Meier, Lorenz, et al. "Pixhawk: A system for autonomous flight using onboard computer vision." in *IEEE international conference on Robotics and automation (ICRA)*, 2011.

[17] http://www.ros.org/